Preprint of the paper
Ripka, P.: Contactless measurement of electric current using magnetic sensors
Technisches Messen. 2019, 86(10), 586-598. ISSN 0171-8096.

Contactless measurement of electric current using magnetic sensors

Pavel Ripka

Czech Technical University in Prague, Czechia
ripka@fel.cvut.cz

Abstract:

We review recent advances in magnetic sensors for DC/AC current transducers, especially novel AMR sensors and integrated fluxgates, and we make critical comparison of their properties. Most contactless electric current transducers use magnetic cores to concentrate the flux generated by the measured current and to shield the sensor against external magnetic fields. In order to achieve this, the magnetic core should be massive. We present coreless current transducers which are lightweight, linear and free of hysteresis and remanence. We also show how to suppress their weak point: crosstalk from external currents and magnetic fields.

Keywords:

Current sensor, Hall, AMR, fluxgate, current transformer

1. Introduction

Measurements of electric current at multiple points are required for modern applications such as smart grids [1], smart buildings, power conversion and electric drives [2], [3], and the car industry. Even if the measured current is at powerline frequency, it often contains a DC component and higher harmonics. The DC component can be of geomagnetic origin [4], induced from DC power lines [5], or injected from transformerless inverters [6]. Higher harmonics usually come from inverters and from other power electronic devices.

It is not always possible to measure the current using a shunt resistor. Although some shunt modules provide galvanic insulation, they cannot be used at high voltages. In addition, the shunt size and power dissipation become impractical when large currents are to be measured. Contactless transducers based on magnetic sensors are therefore an attractive solution.

This paper concentrates on advances in current sensors in the period of almost a decade since [7] and [8] were published. In Section 2, we review the magnetic sensors used in current transducers. An overview of current transducers with a ferromagnetic core is presented in Section 3, and in Section 4 we describe in detail coreless current transducers based on magnetic sensors.

The new definition of the ampere, valid from 20 May 2019, is based on the elementary charge instead of the force. This is a fundamental change in the definition, but it will have no effect on industry.

2. Magnetic sensors used in current transducers

2.1 Sensor parameters and requirements

The general sensor parameters are sensitivity, linearity error, offset and the stability of these parameters with temperature and in time. Parameters specific for magnetic sensors are hysteresis, perming and geometrical selectivity. Hysteresis is usually defined for current changing between the maxima of the full-scale range. Perming refers to the change in the sensor offset after an overload shock caused by a strong external magnetic field or a strong measured DC current. Geometrical selectivity includes sensitivity to the position of the measured conductor as well as the crosstalk from the non-measured currents and the influence of the external magnetic fields [9].

Applications in switching power converters require a large frequency range from dc up to MHz. The sensors should be immune to the rapid changes and large gradients of the electric field that are present in the vicinity of fast switching power devices.

Industrial requirements include environmental resistance, small size, low weight and low price. Sensors should also be easy to install, if possible without interrupting the operation of the current conductor. Low power consumption is required, especially for application in wireless sensor network nodes [10].

First we describe the main types of magnetic sensors, and we discuss their properties and their application potential for electric current transducers. The important parameters of typical industrial magnetic sensors are then summarized in Table 1.

2.2 Hall sensors

The basics of Hall sensors are described in the classical book by Popovic [11]. The most popular Hall sensors are manufactured in silicon CMOS technology. CMOS Hall sensors have a large offset and temperature offset drift, but these can be effectively reduced by spinning techniques. The main advantages of Hall sensors are their large range up to 2 T and their low price.

An example of an advanced programmable Hall sensor is Infineon TLE4997. This smart device has internal digital processing, but it also provides synthetic analog output. The parameters of the device are shown in Table 1.

Using GaAs-based quantum-well Hall-effect technology together with the spinning current technique, offset below 100 nT was achieved [12]. The device has 30 nT detectivity with white noise spectrum down to 60 mHz, close to the Johnson–Nyquist thermal noise.

A broadband, fully-integrated Hall-effect-based current sensor for power applications such as motor drivers and power converters was presented in [3]. Minimum offset of 350 µT is reached for spinning frequencies below 1 MHz. For spinning current frequency of 16 MHz, the bandwidth for the current measurement is 1 MHz.

Sentron CSA-1 is an advanced CMOS integrated Hall sensor with internal magnetic concentrators. The sensor bandwidth is 100 kHz. Applications of the CSA-1 Hall sensor for current measurement are described in [13]. The Hall Sensor microsystem with integrated calibration coils for contactless current measurement achieved sensitivity drift lower than 80 ppm/°C. The offset drifts less than 300 nT/°C, and the nonlinearity is less than ±0.08% [14].

Realization and optimization of gradiometric current transducers based on Hall effect sensors is described in [15] and [16]. Three integrated 2-axis Hall sensors were used to calibrate the conductor position in the yokeless transducer [17].

The main weak point of industrial Hall-based current sensors is their low zero stability, due to the Hall sensor offset: the typical offset drift of a 50 A sensor is 600 mA in the 0–70°C range. This parameter is 20 times worse than the parameter of fluxgate-type current sensor modules.

2.2 Magnetoresistors

The fundamentals of magnetoresistors are covered by the classical book by S. Tumanski [18]. Recent advances in the development of industrial magnetoresistors have been described in [19]. AMR sensors are best suited for linear applications. Their characteristics are linearized by deflecting the direction of the current 45° from the sensing axis with the use of so-called barberpole geometry. This is done without any field bias, so that the resulting characteristics are stable. The offset is stabilized by the flipping technique.

Honeywell HMC 1001 is an example of a precise AMR sensor, while KMZ 51, produced by NXP (formerly Philips) is less precise but cheaper. Both of these sensors have integrated flipping and feedback coils. A disadvantage is their limited range of only 200 μT. The sensitivity and the range of AMR sensors can be adjusted by the thickness of the magnetic core. A limiting factor is that for proper operation the core should stay in the single-domain state. The STMicroelectronics' LIS3MDL is a three-axis AMR sensor with digital output which operates to 1.6 mT, but with lower accuracy: the manufacturer does not specify the offset stability with temperature.

Some authors have reported on the use of AMR sensors with external bias magnets. A weak point of this design is the poor stability of the bias field with temperature and in time [20]. An application of an AMR sensor array in a circular transducer is reported in [21].

The frequency characteristics of AMR current sensors can be extended by using planar magnetic concentrators made of a conductive non-ferromagnetic material. Due to the effect of eddy currents, the magnetic field lines are deflected towards the sensor, which compensates the drop in sensitivity at high frequencies. A bandwidth of 400 kHz is achieved [22].

Giant-Magnetoresistance (GMR) sensors are small in size and they have broad bandwidth, but they suffer from poor linearity, typically of 2 to 6%, and large hysteresis of 2 to 15% [23]. A GMR-based voltage and current transducer achieved 0.2% error for current values up to ±100 A in the temperature range from -30°C to 90°C. [24]. Monolithic integration of GMR sensors with standard CMOS process current sensing is possible [25]. The sensor is used to measure the buried electrical current inside the chip.

George [26] describes current sensing by a GMR magnetic sensor. The popular AA002-02 from NVE Corporation, USA, was used. This sensor IC has a linear range of 150 to 1050 μT. The sensor was therefore biased, using a permanent magnet, to operate around 600 μT. High linearity can be achieved with this sensor, if the measuring range near the bias point is small. This solution brings a problem with the stability of the bias magnet.

TMR sensors have also been used in current sensing [27] [28], but with accuracy that is limited by the non-linearity, hysteresis and poor offset stability of these devices (Table 1).

2.3 Fluxgate sensors

Low-Cost Self-Oscillating Fluxgate Transducers have also been used to measure high currents [29]. The first microfluxgate sensor on the market was developed by Texas Instruments for current sensing applications [30]. Microfluxgate sensors use pulse excitation to reduce power consumption [31]. Microfluxgates have been used for busbar current sensors with the sensors inside the busbar and with the sensors around the busbar.

2.3. Magnetooptical current sensors

These devices are based on the Kerr effect in optical fibers or in the bulk material: the polarization plane rotates by angle proportional to the magnetic field. These sensors are ideal for high-voltage applications, but their resolution is limited by noise and drift. The achievable accuracy is 0.1% for currents from 1 kA to 500 kA.
Fiber-optic current and voltage sensors for electric power transmission systems were recently reviewed by Bohnert [32]. These sensors often use a phase modulation technique that was originally developed for fiber-optic gyroscopes to measure the phase shift between the left and right circular light beams in a fiber coil around the measured conductor. The accuracy depends on the fibre quality [33] and also on the optical connectors [34].

Fiber-optic current and voltage sensors suffer from magnetic crosstalk caused by non-homogeneity of the fiber. By proper design, the crosstalk of 0.3% from the external conductor at a distance of 30 cm can be reduced to 0.002% [35]

A clamp-on optical current sensor based on the Faraday effect in a low birefringence, high Verdet constant, 8 cm long SF57 Schott glass prism was described in [36]. The achieved range is 65 kA, and 0.1% accuracy was achieved for a 1.2 kA current. For this range, the maximum error was 11 mA.

Direct current imaging can also be performed with the use of a magneto-optical sensor [37].

2.4. Other

In this section, we describe other principles that have appeared in the literature, but which have very limited application potential.

A resonant MEMS gradiometer based on the Lorentz force would be suitable for measuring large currents, as it has a large dynamic range, but its resolution is limited by 3 μT noise [38].

Magnetic field sensors based on the force effect on a permanent magnet have been used for current sensing. Simple devices such as [39], [40], [41], [42] suffer from poor sensitivity and poor accuracy. However, the old definition of the ampere was based on force, and the Kibble balance was a very accurate instrument. The passive MEMS DC Electric Current Sensor [43, 44] is also based on the force applied to a micromagnet, which is measured by PZT cantilevers.

Magnetoelectric sensors have received significant attention recently [45] [46]. They are based on coupling between magnetostrictive and piezoelectric properties. The highest response is from laminates made of sheets rather than from multilayer thin-film devices. Elastic coupling makes these

devices temperature-dependent. Devices using Terfenol-D alloy with a gigantic magnetostriction coefficient need a large bias field, which makes them unstable [47], [48], [49].

GMI sensors have also been used for current measurement [50, 51]. The main problems with GMI are perming, if the device is not periodically demagnetized, and also temperature dependence [52]. A GMI current sensor can be coupled with an SAW transponder to form a wireless current sensor suitable for applications that do not require high accuracy [53].

Magnetostriction is used in Fiber Bragg Grating sensors [54], [55], and in sensors based on the Rayleigh backscattering spectral shift in optical fibers [56]. However, the performance of these devices is still much worse than that of magnetooptical fiber sensors. A magnetostrictive element can also be coupled to an SAW sensing device [57], [58].

SQUID can be used as an incremental current sensor with fA resolution [59], [60]. Cryogenic current comparators are used in electric current metrology.

	TI DRV425	Honeywell HMC1001	KMZ 51 (NXP)	AA002 NVE	Infineon TLE 4997	Sentron CSA/1V	MultiDimension TMR2301
technology	integrated fluxgate	AMR module Open loop, S/R on	AMR sensor	GMR sensor	Hall	Hall with concentrators	TMR
Noise @ 1 Hz	5 nT	.5 nT	2 nT/	6 nT	100 µT rms		100 nT
Noise @ 100 Hz	1 nT	0.2 nT	0.3 nT			125 nT	
Offset	500 nT < 8 µT	20 nT < 60 nT	60 µT/		100 µT < 1 mT	800 µT	2,5 mT
Offset drift nT/K	5	20	240		5000	800	
Gain drift (ppm/K)	+/- 7	- 600		+/- 3 000	20 % -40 to + 125 °C	+/- 200	+/- 1100
Hysteresis (10 mT sweep)	1.4 µT (10 mT sw)	0.1 µT < 0.2 µT (200 µT sweep)		40 µT 4 %			200 µT (20 mT sweep)
Linearity	0.1 %	0.1 % (< 2 %)		2 %		0.5 % (0.2% for B<7.5 mT	1.5 % for B<20 mT
Range	2 mT	0.2 mT	0.2 mT	1 mT	200 mT	10 mT	50 mT
Supply current	5 mA to 30 mA	27 < 35 mA	5 mA to 30 mA				0,2 mA
Price	3 US$	HMC1001: 27 US$ HMR2300: 300 US$	10 US$				

Tab. 1 Parameters of magnetic sensors available on the market

3. Current sensors with a core

Most contactless electric current sensors use magnetic cores to concentrate the flux generated by the measured current and to shield the sensor against external magnetic fields. The flux in the high-permeability core or yoke does not depend on the position of the measured current conductor. Some sensors are produced with split cores in the form of openable clamps. This allows the sensor to be mounted without interrupting the measured current circuit.

3.1 Current sensors using a gapped core

If the core has narrow radial airgap, the field intensity H in the airgap is the same as in the core. This field is measured either by a Hall sensor, by a magnetoresistor or by a microfluxgate. The sensing direction of a Hall sensor is perpendicular to the sensing layer, so the sensor can be slim and it can be inserted into a small airgap. Even if the airgap is short, it creates non-homogeneity of the magnetic circuit and degrades the immunity against the displacement of the measured current and against the external magnetic fields. The sensing direction of microfluxgates and magnetoresistors is in the plane of the sensing layer, so they should be inserted into the slot (Fig. 1). The sensor has integrated excitation and signal processing electronics, including the feedback amplifier (Fig. 2).

The field in the airgap is temperature-dependent due to the magnetostriction, the thermal expansion and the temperature dependence of the core permeability. Methods for achieving self-compensation are discussed in [61]. Some sensors may have multiple gaps to achieve symmetry or to measure the currents in the power cord [62].

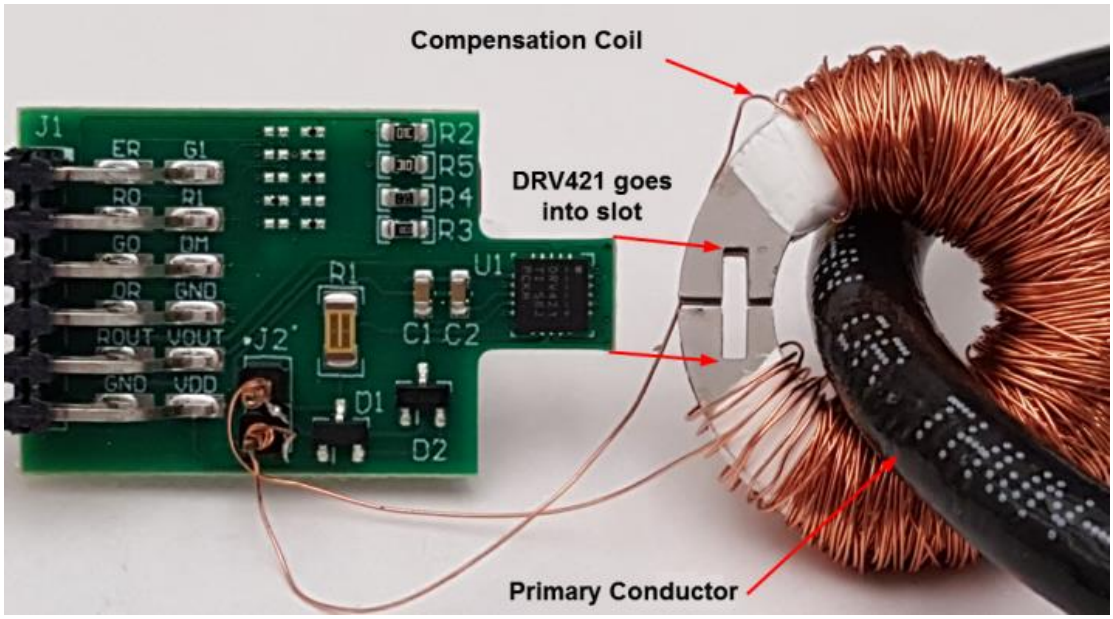

Fig. 1 Prototype of the feedback compensated electric current sensor. The microfluxgate serves as a zero detector. In the final version, the compensation coil is wound around the whole core and the inserted sensor is not visible (Texas Instruments)

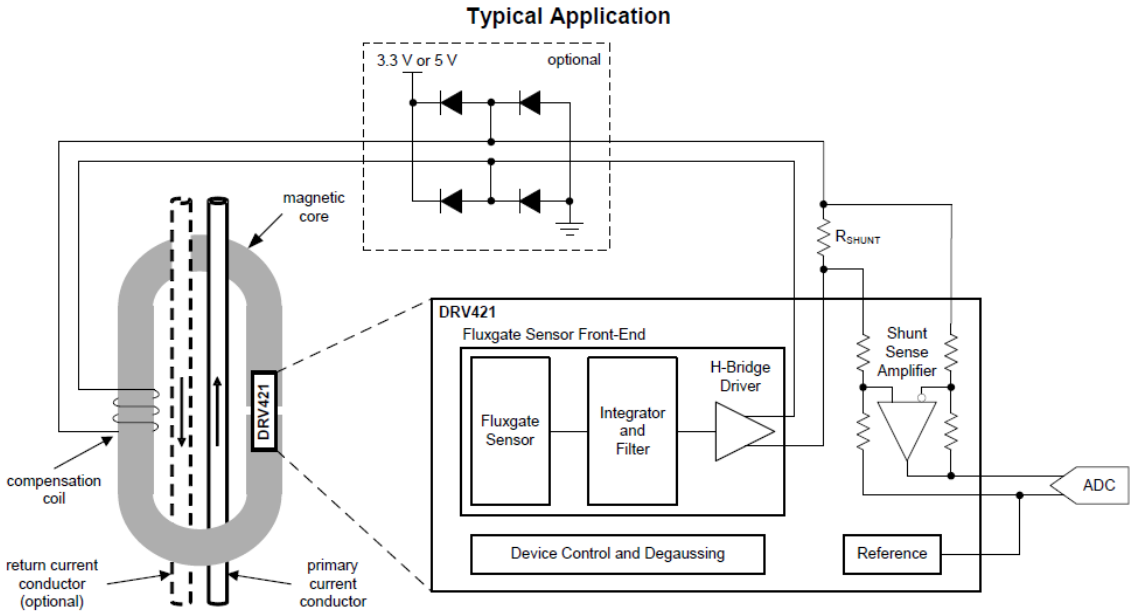

Fig. 2 Schematics of the feedback compensated microfluxgate current sensor with a magnetic core (Texas Instruments)

3.2. Current transformers, Rogowski coils and fluxgate current sensors

Current transformers use a core without an airgap. They are simple, robust devices, and require no external power source. They measure only AC currents, and they can be saturated by a DC current component. After they have been magnetized they lose precision, and they need to be demagnetized [63]. Demagnetization can be achieved by increasing the burden [64]. High-Frequency Current Transformers work up to 50 MHz [65].

Some authors propose the use of current transformers with a low cross-sectional area of the core [66]. This approach results in low accuracy, as the main inductance of such transformer is low. If the transformer is made of foil and is wrapped around the measured conductor, the main inductance is even lower, due to the unavoidable airgap. The third source of large error is high resistance of the secondary winding of flexible transformers of this type. A thin core with an airgap is also susceptible to external magnetic fields. Another mistake is to measure the secondary voltage instead of the current [67] . Unloaded secondary voltage depends on the derivative of the primary current, but the sensitivity of a sensor of this type depends on the permeability, which changes with the temperature and the amplitude of the current. These sensors are therefore unstable and non-linear.

Rogowski coils have no ferromagnetic core, but they also measure only AC currents. In order to obtain a field signal, the output of the Rogowski coil needs to be integrated. Each coil should be calibrated together with the integrator. Rogowski coils can be flexible so that they can be easily mounted around the large conductor. Another Rogowski coils are made in PCB technology [68], so that they can be integrated into the laminated busbar [69] (Fig. 3) . They are often used to measure transient and pulse currents. Shielding improves their bandwidth and reduces parasitic capacitive coupling [70]. The B-Dot sensor works on the same principle as a Rogowski coil, using flat coils made of multilayer PCB [71].

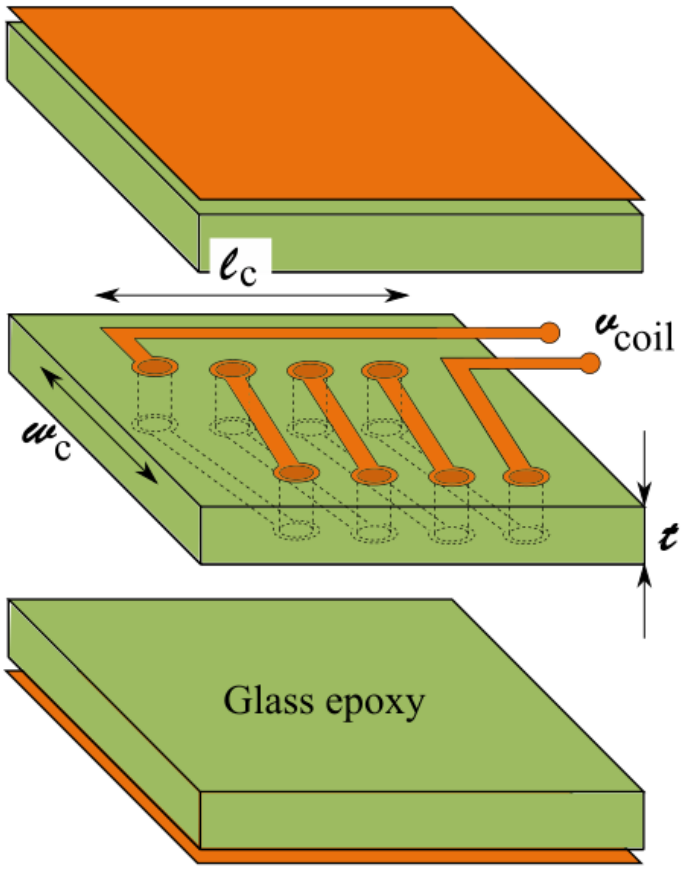

Fig. 3 Rogowski coil integrated into the laminated busbar - after [69]

A fluxgate current sensor has a toroidal core, which is periodically excited to saturation. The DC component in the measured current shifts the magnetization characteristics, and the second harmonics appear in the flux waveform and also in the induced voltage. As the dependence of the second harmonic component voltage on the DC current is non-linear, fluxgate current sensors usually work in the feedback loop compensating the measured DC current to zero. These sensors are also called DC current transformers [72], [73], [74]. We have shown that this mechanism can be used on a standard current transformer by injecting the excitation current into the secondary winding [75].

A fluxgate-based current sensor with a magnetic wire core can measure DC currents up to 5 kA with 0.25% precision [76]. The disadvantage of a low cross-sectional area is low demagnetization and therefore large influence of external fields.

3.3. Disadvantages of sensors with a ferromagnetic core

The use of a magnetic core also brings disadvantages:
1. the magnetic material of the yoke is nonlinear, which causes nonlinearity of the sensor characteristics. It can even be saturated. This can be solved by feedback compensation.

Compensated current sensors also have better temperature stability of the sensitivity. However, these improvements require secondary winding, and there is greater power consumption than for uncompensated sensors.

2. The core needs to be massive in order to have high demagnetization against external fields. This makes the sensor large, heavy and expensive, which can be a limitation for mobile and embedded applications.

3. The core can be intentionally saturated by an external permanent magnet.

4. The core can be permanently magnetized by DC current or by a DC field. Current transformers can be demagnetized by increasing the measured current, or by using extra winding and an external power source. Another option is to increase the transformer burden, which increases the core flux without increasing the current [64]. Gapped core sensors are more resistant to perming, but only a few gapped core sensors have a demagnetization circuit.

4. Coreless current transducers with magnetic sensors

Coreless current transducers (sometimes referred to as yokeless) measure the current through its magnetic field. Due to the absence of a core they are linear, small in size and lightweight.

The sensitivity of coreless current transducers depends on the permeability of the current conductor. This means that if a ferromagnetic conductor is used instead of a copper or aluminum conductor, the transducer must be recalibrated [77].

4.1 single sensor solution

According to the Ampere law, current I in a long straight conductor at a distance d creates field H = I/2πd. This assumes that the return conductor at very long distance. When a single sensor is used, the external field is not suppressed. If the measured current is at a distance of 5 cm and the same external current is at a distance 1 m (this may be the return conductor), the total field is

$$H = H_0 + \Delta H = \frac{I}{2\pi \cdot 0.05\mathrm{m}} + \frac{I}{2\pi \cdot 1\mathrm{m}} \ (\mathrm{A/m})$$

and thus the relative error

$$\delta H = \frac{\Delta H}{H_0} \cdot 100\% = 5\ \%$$

In order to suppress this type of error, the distance d is often minimized. This brings high sensitivity to changes of d with time and temperature.

4.2 gradiometric transducers

A gradiometric transducer calculates the difference between the readings of two sensors in gradiometric configuration. This suppresses the external homogeneous magnetic field.

If the sensors are symmetrically positioned on both sides of the conductor (Fig. 4a), for the same dimensions as in our example we can write for measured fields:

$$H_1 = \frac{I}{2\pi \cdot 0.05\mathrm{m}} + \frac{I}{2\pi \cdot 1\mathrm{m}} \ (\mathrm{A/m})$$

$$H_2 = -\frac{I}{2\pi \cdot 0.05\text{m}} + \frac{I}{2\pi \cdot 1.1\text{m}}\ (\text{A/m})$$

$$H_1 - H_2 = \frac{I}{\pi \cdot 0.05\text{m}} + \frac{I}{2\pi \cdot 1\text{m}} - \frac{I}{2\pi \cdot 1.1\text{m}}\ (\text{A/m})$$

And the error is only δH = 100 (0,5 –0,454)/20 = 0.23 %.

If both sensors are on the same side of the conductor (Fig. 4b),

$$H_1 = \frac{I}{2\pi \cdot 0.05\text{m}} + \frac{I}{2\pi \cdot 1\text{m}}\ (\text{A/m})$$

$$H_2 = \frac{I}{2\pi \cdot 0.1\text{m}} + \frac{I}{2\pi \cdot 0.95\text{m}}\ (\text{A/m})$$

and the error can be calculated similarly: δH = 100 (0,5 –0,526)/5 = 0.52 %.

This means that the symmetrical configuration in our example has fourfold higher sensitivity and twice the suppression of the external current.

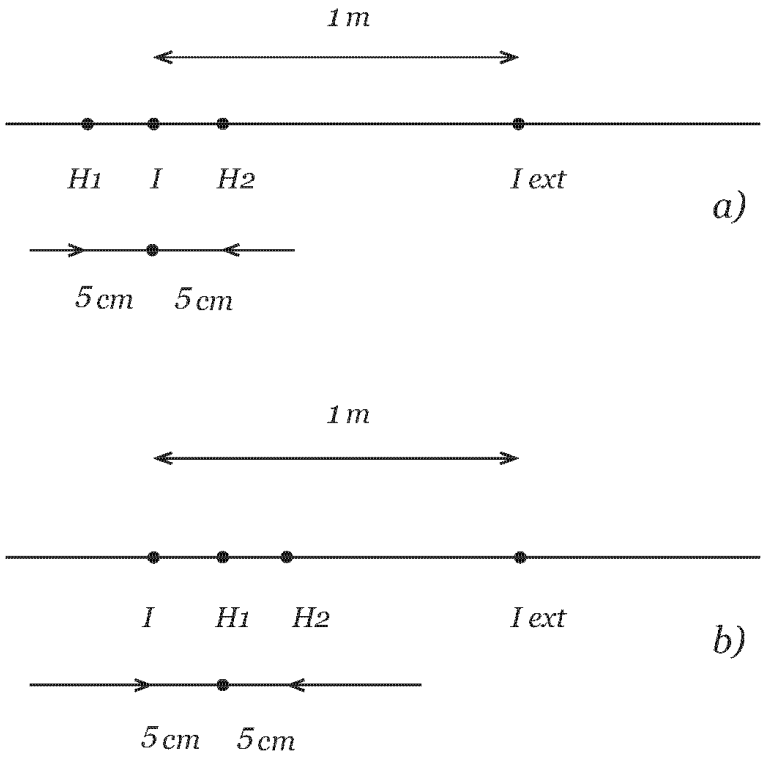

Fig. 4 gradiometric current sensor: a) symmetrical, b) single-side

The realization and the optimization of gradiometric current transducers based on Hall effect sensors are described in [15] and [16]. The influence of the external current on the gradiometric busbar sensor is analyzed in [78]. Complete suppression of external fields and gradients requires more sensors [79]. For measurements of currents up to the 50 A range, gradiometric sensors with a short base are often positioned inside the folded conductor [80], [16].

4.3. circular and rectangular sensor arrays

Circular arrays of Hall sensors have received significant attention [81-84] . The main advantage of a circular array is that it provides much better suppression of external currents than a differential sensor configuration. Suppression well below 0.1 % can be achieved if the sensors are calibrated for sensitivity and geometrical misalignment.

The error caused by the position of the conductor in a circular array is analysed using AMR sensors in [85], using TMR sensors in [27], and using Hall sensors in [86]. When eight uncalibrated AMR sensors were used, the error caused by the current position was ±0.4%, and after calibration and correction the error decreased to ±0.06%.

A sensor based on a circular array of microfluxgate sensors was described in [87]. We have developed a similar transducer of rectangular shape [88]. The sensor location and also the magnetic field lines around the rectangular busbar are shown in Fig. 5, and a realization of a prototype is shown in Fig. 6. Rejection of the external field depends on the number of sensors: Fig. 6 shows the error of a rectangular current transducer caused by the external current, if 8, 10 or all 16 sensors are employed. A rectangular array of microfluxgates performs better than an industrial transducer based on an uncompensated Hall sensor in the airgap of a ferromagnetic core [88].

A coreless current probe for a conductor with reduced access was described in [26].

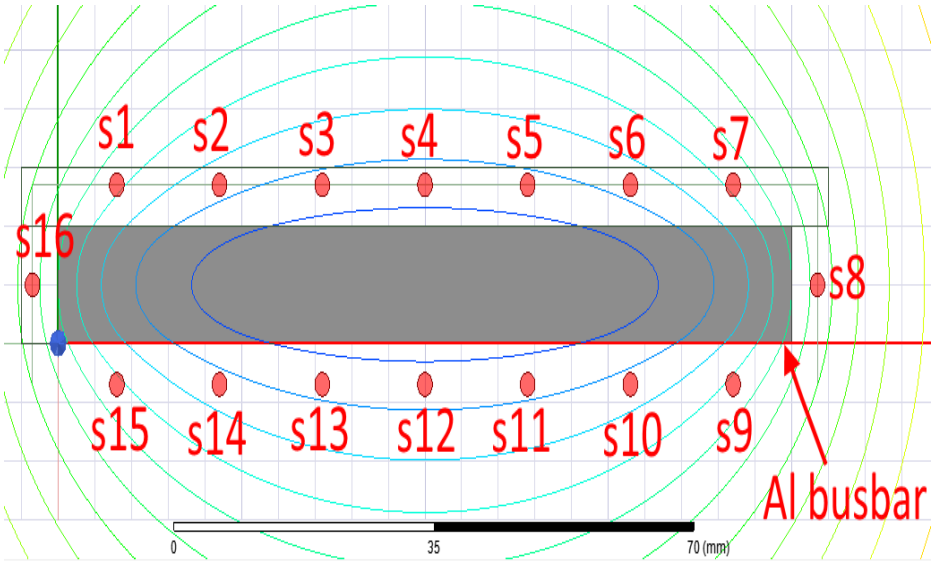

Fig. 5 Rectangular current transducer - location of the sensors [88]

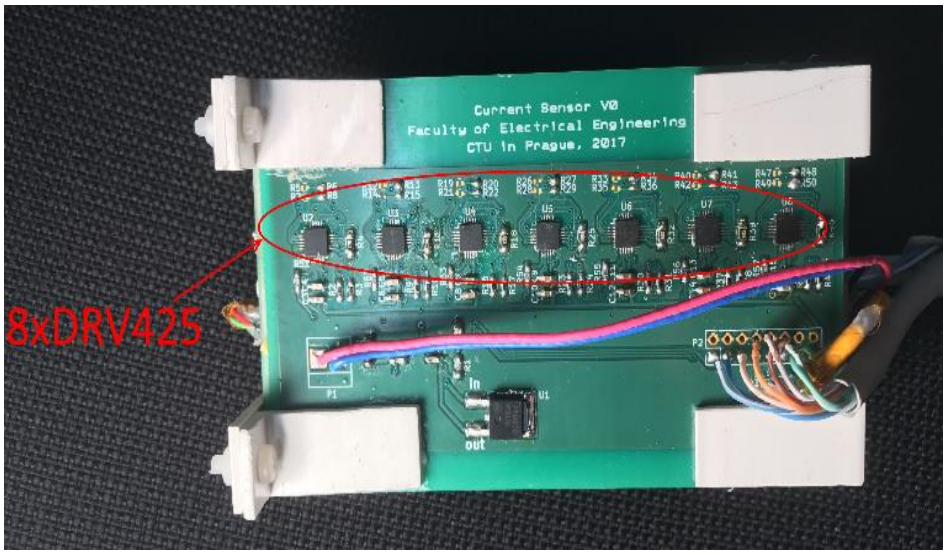

Fig. 6 prototype of the rectangular current transducer using 16 microfluxgate sensors around the measured conductor [88]

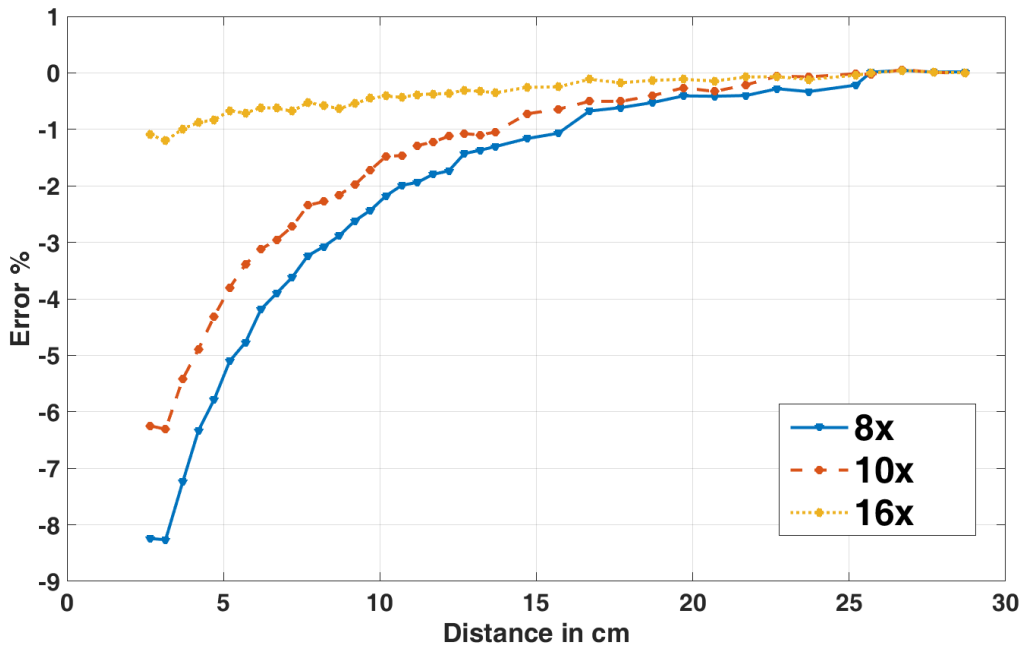

Fig. 7 Error of the rectangular current transducer caused by external current, if 8, 10 or all 16 sensors are employed. [88]

4.4. sensors inside the busbar

The magnetic field in the vicinity of a large current is high: if we want to measure a 10 kA current with a microfluxgate sensor with 2 kA/m range, the sensor should be positioned at a minimum distance of 1000/(2π*2000) = 0.8 m. For a precise AMR sensor with 200 A/m, the minimum distance is 8 m. This can be solved by using Hall sensors with a larger range, but with much worse accuracy and temperature dependence. An elegant solution is to insert a gradiometric sensor inside a hole drilled in the busbar [89], (Fig. 8). The field distribution calculated by FEM simulation is shown in Fig.

9. The sensitivity and the range of the current transducer can be adjusted by changing the distance between sensors H_1 and H_2 in the gradiometric pair.

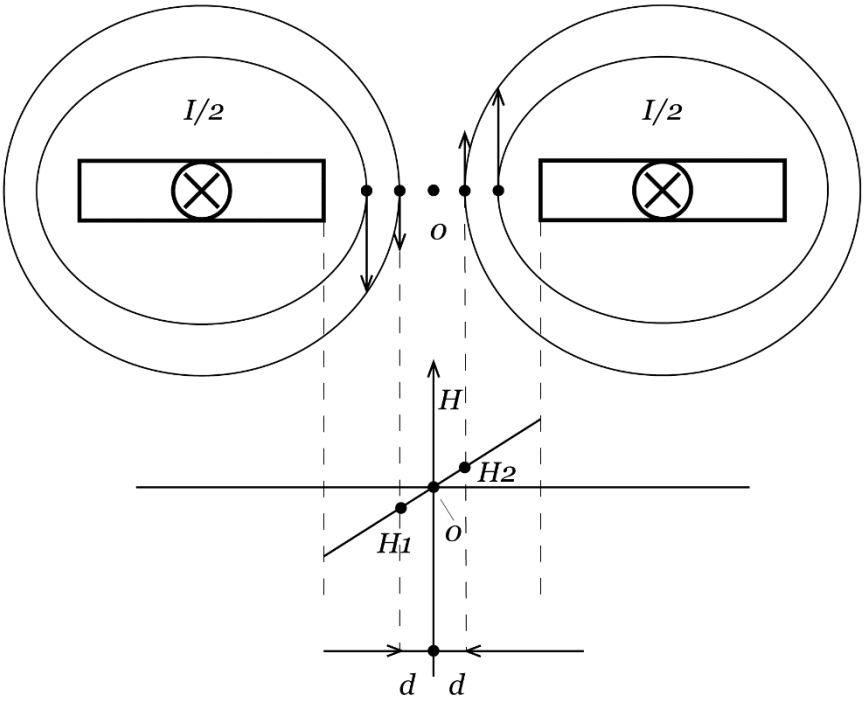

Fig. 8 Busbar with a pair of gradiometric sensors inside the hole

For this type of gradiometric sensor, there is also limited rejection of the signal from external currents: current at a distance of 14 cm is suppressed only by a factor of 66 [78]. This can be improved to 1300 by using a larger number of sensors [79]. A prototype of this transducer with 5 sensors is shown in Fig. 10.

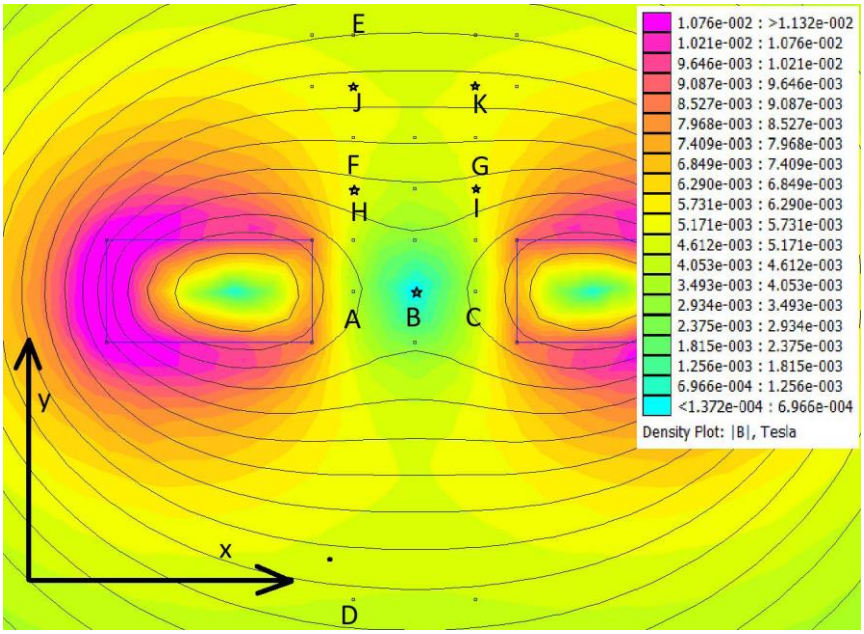

Fig. 9 Field distribution on a cross section of a busbar with a hole. The dc current value for this simulation was 1000 A. The current transducer is marked by stars. [79]

Fig. 10 High current transducer with 5 microfluxgate sensors inside the busbar [79]

4.5 3-phase current transducers

The first attempt to measure 3-phase electric current in overhead lines using coreless transducers was made by Bernieri [90]. In order to improve the interference rejection, Chen added semicircular shielding elements to each gradiometric sensor couple [91]. We suggested an improved geometry, and we used microfluxgate sensors. When 8 sensors are used, the crosstalk between the phases is completely suppressed, and external magnetic field gradients are compensated up to the 4th order [92].

A low-cost multicoil-based transducer for three-phase overhead lines achieved 5% error for distances up to 50 cm [93]. For overhead transmission lines with bundle wires, even individual currents can be calculated from the reading of the sensor field [94].

4.6. Distant measurement of electric currents

Ground sensors can be used to measure the currents in HVDC overhead transmission lines [95]. The authors report that the main source of error is the 5% uncertainty of the actual position of the wire. However the TMR sensor that was used has an offset specification of +/- 2,5 mT, which represents current uncertainty of 40 kA (!) at a typical distance of 40 m. This means that the proposed concept should be used with other magnetic sensors with much better offset specifications.

Undersea cables are localized by submarines equipped with two tri-axial magnetometers [96]. A robust magnetic tracking method has been developed for an AUV operating in the presence of sensor noise and ocean currents [97].

On-Site Non-Invasive Current Monitoring of Multi-Core Underground Power Cables With a Magnetic-Field Sensing Platform at a Substation is presented in [98].

4.6. Measurements of currents in multiwire cables

Individual currents in multiwire cables can be measured with the use of a circular sensor array. 8% accuracy was achieved for 6 sensors [99]. Similarly as in the case of single current sensors, immunity against external fields can be increased by using differential methods: a differential array showed crosstalk errors of less than 5% if the distance of the source of interference was over 200 mm [100].

5. Conclusions

Circular or rectangular coreless current transducers use an array of magnetic sensors to approximate the closed-line integral in Ampere's circuital law. Using 6 to 12 sensors brings independence of the position of the measured conductor and high resistance against external fields. Using microfluxgate sensors, we achieved better performance than for an industrial transducer based on an uncompensated Hall sensor in the airgap of a ferromagnetic core.
More compact, simple gradient sensors are used for less demanding applications. To measure large current, sensors can be inserted into the hole in the busbar.

Funding:

This work was supported by the Grant Agency of the Czech Republic within the New Methods for the Measurement of Electric Currents" project (GACR 17-19877S).

References

[1] Salman, and K. Salman, *Introduction to the Smart Grid*: The Institution of Engineering and Technology, 2017.

[2] J. M. Choe, Y. J. Lee, Y. Cho *et al.*, "A Performance Comparison of the Current Feedback Schemes with a New Single Current Sensor Technique for Single-Phase Full-Bridge Inverters," *Journal of Power Electronics,* vol. 16, no. 2, pp. 621-630, Mar, 2016.

[3] M. Crescentini, M. Marchesi, A. Romani *et al.*, "A Broadband, On-Chip Sensor Based on Hall Effect for Current Measurements in Smart Power Circuits," *Ieee Transactions on Instrumentation and Measurement,* vol. 67, no. 6, pp. 1470-1485, Jun, 2018.

[4] A. Pulkkinen, E. Bernabeu, A. Thomson *et al.*, "Geomagnetically induced currents: Science, engineering, and applications readiness," *Space Weather-the International Journal of Research and Applications,* vol. 15, no. 7, pp. 828-856, Jul, 2017.

[5] S. H. Yang, G. Zhou, and Z. N. Wei, "Influence of High Voltage DC Transmission on Measuring Accuracy of Current Transformers," *Ieee Access,* vol. 6, pp. 72629-72634, 2018.

[6] G. Buticchi, G. Franceschini, E. Lorenzani *et al.*, *A Novel Current Sensing DC Offset Compensation Strategy in Transformerless Grid Connected Power Converters*, New York: Ieee, 2009.

[7] P. Ripka, "Electric current sensors: A review," *Measurement Science and Technology,* vol. 21, no. 11, 2010, 2010.

[8] S. Ziegler, R. C. Woodward, H. H. C. Iu *et al.*, "Current Sensing Techniques: A Review," *Ieee Sensors Journal,* vol. 9, no. 4, pp. 354-376, Apr, 2009.

[9] P. Ripka, P. Kaspar, and J. Saneistr, "Geometrical selectivity of current sensors," *Przeglad Elektrotechniczny,* vol. 88, no. 5A, pp. 38-39, 2012.

[10] F. Adamo, F. Attivissimo, A. Di Nisio *et al.*, *Comparison of Current Sensors for Power Consumption Assessment of Wireless Sensors Network Nodes*, New York: Ieee, 2017.

[11] R. S. Popovic, *Hall Effect Devices*: CRC Press, 2003.

[12] V. Mosser, N. Matringe, and Y. Haddab, "A Spinning Current Circuit for Hall Measurements Down to the Nanotesla Range," *Ieee Transactions on Instrumentation and Measurement,* vol. 66, no. 4, pp. 637-650, Apr, 2017.

[13] M. Blagojevic, U. Jovanovic, I. Jovanovic *et al.*, "CORELESS OPEN-LOOP CURRENT TRANSDUCERS BASED ON HALL EFFECT SENSOR CSA-1V," *Facta Universitatis-Series Electronics and Energetics,* vol. 29, no. 4, pp. 489-507, Dec, 2016.

[14] A. Ajbl, M. Pastre, and M. Kayal, "A Fully Integrated Hall Sensor Microsystem for Contactless Current Measurement," *Ieee Sensors Journal,* vol. 13, no. 6, pp. 2271-2278, Jun, 2013.

[15] M. Blagojevic, U. Jovanovic, I. Jovanovic *et al.*, "Realization and optimization of bus bar current transducers based on Hall effect sensors," *Measurement Science and Technology,* vol. 27, no. 6, Jun, 2016.

[16] M. Blagojevic, U. Jovanovic, I. Jovanovic *et al.*, "Folded bus bar current transducer based on Hall effect sensor," *Electrical Engineering,* vol. 100, no. 2, pp. 1243-1251, Jun, 2018.

[17] J. Y. C. Chan, N. C. F. Tse, and L. L. Lai, "A Coreless Electric Current Sensor With Circular Conductor Positioning Calibration," *Ieee Transactions on Instrumentation and Measurement,* vol. 62, no. 11, pp. 2922-2928, Nov, 2013.

[18] S. Tumanski, *Thin Film Magnetoresistive Sensors*: Press, 2001.

[19] L. Jogschies, D. Klaas, R. Kruppe *et al.*, "Recent Developments of Magnetoresistive Sensors for Industrial Applications," *Sensors,* vol. 15, no. 11, pp. 28665-28689, Nov, 2015.

[20] Z. H. Zhang, O. Syuji, A. Osamu *et al.*, "Development of the Highly Precise Magnetic Current Sensor Module of +/-300 A Utilizing AMR Element With Bias-Magnet," *Ieee Transactions on Magnetics,* vol. 51, no. 1, pp. 5, Jan, 2015.

[21] P. Mlejnek, and P. Ripka, "AMR yokeless current sensor with improved accuracy," *Proceedings of the 30th Anniversary Eurosensors Conference - Eurosensors 2016*, Procedia Engineering I. Barsony, Z. Zolnai and G. Battistig, eds., pp. 900-903, 2016.

[22] S. J. Nibir, and B. Parkhideh, "Magnetoresistor with Planar Magnetic Concentrator as Wideband Contactless Current Sensor for Power Electronics Applications," *Ieee Transactions on Industrial Electronics,* vol. 65, no. 3, pp. 2766-2774, Mar, 2018.

[23] A. Bernieri, G. Betta, L. Ferrigno *et al.*, "Improving Performance of GMR Sensors," *Ieee Sensors Journal,* vol. 13, no. 11, pp. 4513-4521, Nov, 2013.

[24] F. Xie, R. Weiss, and R. Weigel, "Giant-Magnetoresistance-Based Galvanically Isolated Voltage and Current Measurements," *Ieee Transactions on Instrumentation and Measurement,* vol. 64, no. 8, pp. 2048-2054, Aug, 2015.

[25] A. De Marcellis, C. Reig, M. D. Cubells-Beltran *et al.*, "Monolithic integration of GMR sensors for standard CMOS-IC current sensing," *Solid-State Electronics,* vol. 135, pp. 100-104, Sep, 2017.

[26] N. George, and S. Gopalakrishna, "Development of a New Low-Cost and Reliable Core-Less Current Probe for Conductor With Reduced Access," *Ieee Sensors Journal,* vol. 17, no. 14, pp. 4619-4627, Jul, 2017.

[27] H. Yu, Z. Qian, H. Y. Liu *et al.*, "Circular Array of Magnetic Sensors for Current Measurement: Analysis for Error Caused by Position of Conductor," *Sensors,* vol. 18, no. 2, pp. 12, Feb, 2018.

[28] M. Dabek, P. Wisniowski, P. Kalabinski *et al.*, "Tunneling magnetoresistance sensors for high fidelity current waveforms monitoring," *Sensors and Actuators a-Physical,* vol. 251, pp. 142-147, Nov, 2016.

[29] N. Wang, Z. H. Zhang, Z. K. Li *et al.*, "Design and Characterization of a Low-Cost Self-Oscillating Fluxgate Transducer for Precision Measurement of High-Current," *Ieee Sensors Journal,* vol. 16, no. 9, pp. 2971-2981, May, 2016.

[30] D. W. Lee, M. Eissa, A. Gabrys *et al.*, "Fabrication and Performance of Integrated Fluxgate for Current Sensing Applications," *Ieee Transactions on Magnetics,* vol. 53, no. 11, pp. 4, Nov, 2017.

[31] P. Ripka, S. O. Choi, A. Tipek *et al.*, "Pulse excitation of micro-fluxgate sensors," *Ieee Transactions on Magnetics,* vol. 37, no. 4, pp. 1998-2000, Jul, 2001.

[32] K. Bohnert, A. Frank, G. M. Muller *et al.*, "Fiber-optic current and voltage sensors for electric power transmission systems," *Fiber Optic Sensors and Applications Xv*, Proceedings of SPIE A. Mendez, C. S. Baldwin and H. H. Du, eds., 2018.

[33] M. Aerssens, F. Descamps, A. Gusarov *et al.*, "Influence of the optical fiber type on the performances of fiber-optics current sensor dedicated to plasma current measurement in ITER," *Applied Optics,* vol. 54, no. 19, pp. 5983-5991, Jul, 2015.

[34] K. Bohnert, C. P. Hsu, L. Yang *et al.*, "Fiber-Optic Current Sensor Tolerant to Imperfections of Polarization-Maintaining Fiber Connectors," *Journal of Lightwave Technology,* vol. 36, no. 11, pp. 2161-2165, Jun, 2018.

[35] S. Cheng, Z. Z. Guo, G. Q. Zhang *et al.*, "Distributed parameter model for characterizing magnetic crosstalk in a fiber optic current sensor," *Applied Optics,* vol. 54, no. 34, pp. 10009-10017, Dec, 2015.

[36] I. M. Nascimento, A. C. S. Brigida, J. M. Baptista *et al.*, "Novel optical current sensor for metering and protection in high power applications," *Instrumentation Science & Technology,* vol. 44, no. 2, pp. 148-162, Mar, 2016.

[37] S. Arakelyan, O. Galstyan, H. Lee *et al.*, "Direct current imaging using a magneto-optical sensor," *Sensors and Actuators a-Physical,* vol. 238, pp. 397-401, Feb, 2016.

[38] Kahr, M., M. Stifter *et al.*, "Dual Resonator MEMS Magnetic Field Gradiometer," *Sensors,* vol. 19, 2019.

[39] G. S. Shan, D. F. Wang, and C. Xia, “Integrated piezoelectric direct current sensor with actuating and sensing elements applicable to two-wire dc appliances: theoretical considerations,” *Measurement Science and Technology,* vol. 30, no. 2, Feb, 2019.
[40] F. S. Delgado, J. P. Carvalho, T. V. N. Coelho *et al.*, “An Optical Fiber Sensor and Its Application in UAVs for Current Measurements,” *Sensors,* vol. 16, no. 11, pp. 8, Nov, 2016.
[41] M. H. B. Junior, A. L. Magalhaes, A. M. Bastos *et al.*, “Piezoelectric ceramic sensor (PZT) applied to electric current measurements,” *Microsystem Technologies-Micro-and Nanosystems-Information Storage and Processing Systems,* vol. 25, no. 2, pp. 705-710, Feb, 2019.
[42] Z. Y. Wu, “A Wide Linearity Range Current Sensor Based on Piezoelectric Effect,” *Ieee Sensors Journal,* vol. 17, no. 11, pp. 3298-3301, Jun, 2017.
[43] D. F. Wang, H. Liu, X. D. Li *et al.*, “Passive MEMS DC Electric Current Sensor: Part II-Experimental Verifications,” *Ieee Sensors Journal,* vol. 17, no. 5, pp. 1238-1245, Mar, 2017.
[44] D. F. Wang, H. Liu, X. D. Li *et al.*, “Passive MEMS DC Electric Current Sensor: Part I-Theoretical Considerations,” *Ieee Sensors Journal,* vol. 17, no. 5, pp. 1230-1237, Mar, 2017.
[45] J. T. Zhang, J. Wu, Q. Yang *et al.*, *An Autonomous Current-sensing System for Electric Cord Monitoring Using Magnetoelectric Sensors*, New York: Ieee, 2017.
[46] N. Castro, S. Reis, M. P. Silva *et al.*, “Development of a contactless DC current sensor with high linearity and sensitivity based on the magnetoelectric effect,” *Smart Materials and Structures,* vol. 27, no. 6, pp. 7, Jun, 2018.
[47] X. R. Guo, X. J. Yu, G. F. Lou *et al.*, "A Wide Range DC Current Sensor Based on Disk-type Magnetoelectric Laminate Composite with a Feedback Circuit," *2017 Ieee Sensors*, IEEE Sensors, pp. 334-336, New York: Ieee, 2017.
[48] G. F. Lou, X. J. Yu, and R. Ban, “A wide-range DC current sensing method based on disk-type magnetoelectric laminate composite and magnetic concentrator,” *Sensors and Actuators a-Physical,* vol. 280, pp. 535-542, Sep, 2018.
[49] M. J. Zhang, and S. W. Or, “Gradient-Type Magnetoelectric Current Sensor with Strong Multisource Noise Suppression,” *Sensors,* vol. 18, no. 2, pp. 16, Feb, 2018.
[50] A. Asfour, J. Nabias, P. S. Traore *et al.*, “Practical Use of the GMI Effect to Make a Current Sensor,” *Ieee Transactions on Magnetics,* vol. 55, no. 1, Jan, 2019.
[51] M. Malátek, P. Ripka, and L. Kraus, “Double-core GMI current sensor,” *IEEE Transactions on Magnetics,* vol. 41, no. 10, pp. 3703-3705, 2005, 2005.
[52] M. Malátek, P. Ripka, and L. Kraus, “Temperature offset drift of GMI sensors,” *Sensors and Actuators, A: Physical,* vol. 147, no. 2, pp. 415-418, 2008, 2008.
[53] V. V. Kondalkar, X. Li, I. Park *et al.*, “Development of chipless, wireless current sensor system based on giant magnetoimpedance magnetic sensor and surface acoustic wave transponder,” *Scientific Reports,* vol. 8, pp. 11, Feb, 2018.
[54] J. H. Han, H. F. Hu, H. Wang *et al.*, “Temperature-Compensated Magnetostrictive Current Sensor Based on the Configuration of Dual Fiber Bragg Gratings,” *Journal of Lightwave Technology,* vol. 35, no. 22, pp. 6, Nov, 2017.
[55] D. H. Kim, and S. H. Kim, “Monitoring of Electric Current by Using a Fiber Bragg Grating Sensor,” *Journal of the Korean Society for Nondestructive Testing,* vol. 37, no. 4, pp. 257-261, Aug, 2017.
[56] Z. Y. Ding, Y. Du, T. G. Liu *et al.*, “Distributed Optical Fiber Current Sensor Based on Magnetostriction in OFDR,” *Ieee Photonics Technology Letters,* vol. 27, no. 19, pp. 2055-2058, Oct, 2015.
[57] J. Tong, Y. N. Jia, W. Wang *et al.*, “Development of a Magnetostrictive FeNi Coated Surface Acoustic Wave Current Sensor,” *Applied Sciences-Basel,* vol. 7, no. 8, pp. 16, Aug, 2017.
[58] W. Wang, Y. N. Jia, X. L. Liu *et al.*, "Performance Improvement of the SAW Based Current Sensor Incorporating a Strip-Patterned Magnetostrictive FeCo Film," *2017 Ieee International Ultrasonics Symposium*, IEEE International Ultrasonics Symposium, New York: Ieee, 2017.

[59] D. Drung, J. Beyer, M. Peters *et al.*, "Novel SQUID Current Sensors With High Linearity at High Frequencies," *Ieee Transactions on Applied Superconductivity,* vol. 19, no. 3, pp. 772-777, Jun, 2009.

[60] D. Drung, J. H. Storm, and J. Beyer, "SQUID Current Sensor With Differential Output," *Ieee Transactions on Applied Superconductivity,* vol. 23, no. 3, pp. 4, Jun, 2013.

[61] Y. K. Xiang, Q. F. Xu, Y. F. Huang *et al.*, "A Ferromagnetic Design for Current Sensor Temperature Characteristics Improvement," *Ieee Sensors Journal,* vol. 18, no. 4, pp. 1435-1441, Feb, 2018.

[62] J. Zhang, Y. M. Wen, and P. Li, "Nonintrusive Current Sensor for the Two-Wire Power Cords," *Ieee Transactions on Magnetics,* vol. 51, no. 11, pp. 4, Nov, 2015.

[63] K. Draxler, and R. Styblikova, "Demagnetization of instrument transformers before calibration," *Journal of Electrical Engineering-Elektrotechnicky Casopis,* vol. 69, no. 6, pp. 426-430, Dec, 2018.

[64] J. Bauer, P. Ripka, K. Draxler *et al.*, "Demagnetization of current transformers using PWM burden," *IEEE Transactions on Magnetics,* vol. 51, no. 1, 2015, 2015.

[65] C. Zachariades, R. Shuttleworth, R. Giussani *et al.*, "Optimization of a High-Frequency Current Transformer Sensor for Partial Discharge Detection Using Finite-Element Analysis," *Ieee Sensors Journal,* vol. 16, no. 20, pp. 7526-7533, Oct, 2016.

[66] N. B. Narampanawe, K. Y. See, J. Zhang *et al.*, "Analysis of Ultra-Thin and Flexible Current Transformer Based on JA Hysteresis Model," *Ieee Sensors Journal,* vol. 17, no. 13, pp. 4029-4036, Jul, 2017.

[67] T. Yamashita, Y. Zhang, T. Itoh *et al.*, "Development of thin film based flexible current clamp sensor using screen-printed coil," *Microsystem Technologies-Micro-and Nanosystems-Information Storage and Processing Systems,* vol. 22, no. 3, pp. 577-581, Mar, 2016.

[68] K. Hasegawa, S. Takahara, S. Tabata *et al.*, "A New Output Current Measurement Method With Tiny PCB Sensors Capable of Being Embedded in an IGBT Module," *Ieee Transactions on Power Electronics,* vol. 32, no. 3, pp. 1707-1712, Mar, 2017.

[69] Y. Kuwabara, K. Wada, J. M. Guichon *et al.*, "Implementation and Performance of a Current Sensor for a Laminated Bus Bar," *Ieee Transactions on Industry Applications,* vol. 54, no. 3, pp. 2579-2587, May-Jun, 2018.

[70] C. Hewson, J. Aberdeen, and Ieee, "An improved Rogowski coil configuration for a high speed, compact current sensor with high immunity to voltage transients," *Thirty-Third Annual Ieee Applied Power Electronics Conference and Exposition*, Annual IEEE Applied Power Electronics Conference and Exposition (APEC), pp. 571-578, New York: Ieee, 2018.

[71] J. G. Wang, D. C. Si, T. Tian *et al.*, "Design and Experimental Study of a Current Transformer with a Stacked PCB Based on B-Dot," *Sensors,* vol. 17, no. 4, Apr, 2017.

[72] S. Veinovic, M. Ponjavic, S. Milic *et al.*, "Low-power design for DC current transformer using class-D compensating amplifier," *Iet Circuits Devices & Systems,* vol. 12, no. 3, pp. 215-220, May, 2018.

[73] G. Velasco-Quesada, M. Roman-Lumbreras, R. Perez-Delgado *et al.*, "Class H Power Amplifier for Power Saving in Fluxgate Current Transducers," *Ieee Sensors Journal,* vol. 16, no. 8, pp. 2322-2330, Apr, 2016.

[74] L. Callegaro, C. Cassiago, and E. Gasparotto, "On the Calibration of Direct-Current Current Transformers (DCCT)," *Ieee Transactions on Instrumentation and Measurement,* vol. 64, no. 3, pp. 723-727, Mar, 2015.

[75] P. Ripka, K. Draxler, and R. Styblíková, "DC-Compensated Current Transformer," *Sensors,* vol. 16, 2016, 2016.

[76] L. Grno, "Magnetic Fiber Integrator and its Application in Precision Noninvasive DC Current Sensor," *Ieee Transactions on Instrumentation and Measurement,* vol. 66, no. 8, pp. 2012-2021, Aug, 2017.

[77] M. Mirzaei, P. Ripka, A. Chirtsov *et al.*, "The effect of conductor permeability on electric current transducers," *Aip Advances,* vol. 8, no. 4, pp. 7, Apr, 2018.

[78] P. Ripka, and A. Chirtsov, "Influence of External Current on Yokeless Electric Current Transducers," *Ieee Transactions on Magnetics,* vol. 53, no. 11, pp. 4, Nov, 2017.
[79] P. Ripka, and A. Chirtsov, "Busbar Current Transducer With Suppression of External Fields and Gradients," *Ieee Transactions on Magnetics,* vol. 54, no. 11, Nov, 2018.
[80] H. Beltran, C. Reig, V. Fuster *et al.*, "Modeling of magnetoresistive-based electrical current sensors: A technological approach," *Ieee Sensors Journal,* vol. 7, no. 11-12, pp. 1532-1537, Nov-Dec, 2007.
[81] K. L. Chen, and N. M. Chen, "A New Method for Power Current Measurement Using a Coreless Hall Effect Current Transformer," *Ieee Transactions on Instrumentation and Measurement,* vol. 60, no. 1, pp. 158-169, Jan, 2011.
[82] W. L. Chen, H. Q. Zhang, L. Chen *et al.*, "Wire-positioning algorithm for coreless Hall array sensors in current measurement," *Measurement Science and Technology,* vol. 29, no. 5, pp. 5, May, 2018.
[83] H. G. Kim, G. B. Kang, and D. J. Nam, "Coreless Hall Current Sensor for Automotive Inverters Decoupling Cross-coupled Field," *Journal of Power Electronics,* vol. 9, no. 1, pp. 68-73, Jan, 2009.
[84] Y. P. Tsai, K. L. Chen, Y. R. Chen *et al.*, "Multifunctional Coreless Hall-Effect Current Transformer for the Protection and Measurement of Power Systems," *Ieee Transactions on Instrumentation and Measurement,* vol. 63, no. 3, pp. 557-565, Mar, 2014.
[85] P. Mlejnek, and P. Ripka, "Off-Center Error Correction of AMR Yokeless Current Transducer," *Journal of Sensors*, pp. 7, 2017.
[86] A. Itzke, R. Weiss, and R. Weigel, "Influence of the Conductor Position on a Circular Array of Hall Sensors for Current Measurement," *Ieee Transactions on Industrial Electronics,* vol. 66, no. 1, pp. 580-585, Jan, 2019.
[87] R. Weiss, R. Makuch, A. Itzke *et al.*, "Crosstalk in Circular Arrays of Magnetic Sensors for Current Measurement," *Ieee Transactions on Industrial Electronics,* vol. 64, no. 6, pp. 4903-4909, Jun, 2017.
[88] A. Chirtsov, P. Ripka, and J. Vyhnanek, "Rectangular Array Current Transducer with Integrated Microfluxgate Sensors," in 2018 IEEE SENSORS, New Delhi, India, 2018, pp. 1-4.
[89] M. F. Snoeij, V. Schaffer, S. Udayashankar *et al.*, "Integrated Fluxgate Magnetometer for Use in Isolated Current Sensing," *Ieee Journal of Solid-State Circuits,* vol. 51, no. 7, pp. 1684-1694, Jul, 2016.
[90] A. Bernieri, L. Ferrigno, M. Laracca *et al.*, "An AMR-Based Three-Phase Current Sensor for Smart Grid Applications," *Ieee Sensors Journal,* vol. 17, no. 23, pp. 7704-7712, Dec, 2017.
[91] Y. F. Chen, Q. Huang, and A. H. Khawaja, "An Interference-Rejection Strategy for Measurement of Small Current Under Strong Interference With Magnetic Sensor Array," *Ieee Sensors Journal,* vol. 19, no. 2, pp. 692-700, Jan, 2019.
[92] P. Ripka, V. Grim, and A. Chirtsov, "3-phase current transducer based on microfluxgate sensors," *Sensors,* vol. submitted.
[93] J. Y. Wu, Z. F. Chen, C. Wang *et al.*, "A Novel Low-Cost Multicoil-Based Smart Current Sensor for Three-Phase Currents Sensing of Overhead Conductors," *Ieee Transactions on Power Delivery,* vol. 31, no. 6, pp. 2443-2452, Dec, 2016.
[94] G. Zhao, J. Hu, S. Zhao *et al.*, "Current Reconstruction of Bundle Conductors Based on Tunneling Magnetoresistive Sensors," *Ieee Transactions on Magnetics,* vol. 53, no. 11, pp. 5, Nov, 2017.
[95] Y. K. Xiang, K. L. Chen, Q. F. Xu *et al.*, "A Novel Contactless Current Sensor for HVDC Overhead Transmission Lines," *Ieee Sensors Journal,* vol. 18, no. 11, pp. 4725-4732, Jun, 2018.
[96] K. Asakawa, J. Kojima, Y. Kato *et al.*, "Design concept and experimental results of the autonomous underwater vehicle AQUA EXPLORER 2 for the inspection of underwater cables," *Advanced Robotics,* vol. 16, no. 1, pp. 27-42, 2002.

[97] C. Y. Yu, X. B. Xiang, L. Lapierre *et al.*, "Robust Magnetic Tracking of Subsea Cable by AUV in the Presence of Sensor Noise and Ocean Currents," *Ieee Journal of Oceanic Engineering,* vol. 43, no. 2, pp. 311-322, Apr, 2018.
[98] K. Zhu, W. Han, W. K. Lee *et al.*, "On-Site Non-Invasive Current Monitoring of Multi-Core Underground Power Cables With a Magnetic-Field Sensing Platform at a Substation," *Ieee Sensors Journal,* vol. 17, no. 6, pp. 1837-1848, Mar, 2017.
[99] G. C. Geng, J. C. Wang, K. L. Chen *et al.*, "Contactless Current Measurement for Enclosed Multiconductor Systems Based on Sensor Array," *Ieee Transactions on Instrumentation and Measurement,* vol. 66, no. 10, pp. 2627-2637, Oct, 2017.
[100] A. Itzke, R. Weiss, T. DiLeo *et al.*, "The Influence of Interference Sources on a Magnetic Field-Based Current Sensor for Multiconductor Measurement," *Ieee Sensors Journal,* vol. 18, no. 16, pp. 6782-6787, Aug, 2018.

Bionote

Pavel Ripka

Czech Technical University in Prague,
Faculty of Electrcal Engineering, Dept. of Measurement
Technicka 2
166 27 Praha 6
Czechia
ripka@fel.cvut.cz

Pavel Ripka is a professor in Measurement Science. 2011-2019 he served as a Dean of the faculty of Electrical engineering. His research topic are magnetic sensors, magnetometers and their applications.